

# Reduction of Amyloid Plaque FP Detections in MR images of the APP Transgenic Mouse Brain using Unsupervised SVM

G. IORDANESCU<sup>1,2</sup>, P. Venkatasubramanian<sup>1,2</sup>, and A. Wyrwicz<sup>1,3</sup>

<sup>1</sup>Center for Basic MR Research, Northshore University HealthSystem, Evanston, Illinois, United States, <sup>2</sup>Pritzker School of Medicine, University of Chicago, Chicago, Illinois, United States, <sup>3</sup>Biomedical Engineering, Northwestern University, Chicago, Illinois, United States

## Introduction

Alzheimer's disease (AD) is linked to increased brain deposition of amyloid-beta peptides in senile plaques. Successful visualization of amyloid deposits in the APP transgenic mouse brain with MR imaging has been reported by several investigators recently. However, there are few reports of methods for the measurement of plaque burden in the mouse brain. The number of plaques, their size and brain distribution depend on the transgenic mouse line and vary with age. In our previous work, we presented a method based on a watershed algorithm [1] and support vector machines (SVM) [2] to segment the AD plaques in mouse MR brain images. The algorithm was used to process ROIs in the subiculum, cortex and hippocampus in images of excised mouse brains. The results showed that amyloid deposits are consistent within same age animals, and increase sharply with age. While the analyzed anatomical areas are significant for AD disease, they show relatively consistent background MR intensity, and thus amyloid plaques can be modeled by only two features (data gradient divergence and local contrast). Here we extend our unsupervised learning approach to reduce the false positive detections (FP) of our plaque analysis algorithm when applied to brain areas with heterogeneous MR intensities.

## Methods

**Transgenic Mice:** 5xFAD transgenic mice coexpressing a total of five FAD mutations [APP K670N/M671L (Swedish) + I716V (Florida) + V717I (London) and PS1 M146L + L286V] were produced in a collaborator's laboratory [3]. Plaques begin to appear in the 5xFAD mouse brain relatively early, at 2 months, and level off at 9 months.

**MR imaging:** Brains fixed in 4% paraformaldehyde were used for imaging. During imaging, brains were immersed in Fomblin (a perfluorinated liquid) to prevent dehydration and reduce magnetic susceptibility gradients. All imaging experiments were performed on a Bruker Avance 14.1T imaging spectrometer fitted with a 100G/cm gradient using a 10 or 20 mm resonator tuned to proton frequency (600MHz). 3D images were acquired using a fast spin-echo (RARE8) pulse sequence and the following imaging parameters: TR/TEeff 2500ms/40ms; pixel size 35µm x 35µm x 35µm.

**FP Analysis:** The plaque segmentation algorithm computes the plaque candidates by using simulated flooding (watersheds) to extract catchment basins (CBs). Image Laplacian  $L(I) = \text{div}(\text{grad}(I))$  and local contrast are then used to compute the candidates features. Plaque detection is formulated as an outlier detection problem of the one-class SVM (OCSVM [4]). OCSVM is an extension of the two class SVM, and it estimates a classification function that encloses a majority of the training prototypes in a feature space. Kernel methods can be used to project the original data space into a high dimensional feature space, such that a linear classification in the latter is equivalent to a nonlinear classification in the former. We use the Radial Basis Function (RBF) kernel,  $k(x; x_i) = e^{-\gamma \|x - x_i\|^2}$ , where  $\gamma$  determines the kernel width [5]. In addition to plaques, there are two other sources of high Laplacians and contrast when analyzing heterogeneous brain areas: blood vessels and other tube like structures (modeled as cylinders) and interfaces. These are processed by using isotropic Gaussian blurring to compute new multiscale features for our plaque detection algorithm: data gradient, and the three eigenvalues of the Hessian matrix of the volume intensity function. The Hessian matrix  $H_{jk}(I) = D_j D_k(I)$  is the square matrix of second-order partial derivatives and its eigenvalues provide a curvature analysis that is independent of the data coordinate system. Similar to plaque detection, our FP reduction algorithm has two training steps. First, an OCSVM model is created by training on a ROI where there are no FP sources. This model will classify as FP any CB that has features different than those in the training ROI. Then, a two class SVM is trained on a ROI where a specific FP is present. The training is performed using the labels created by the OCSVM classifier. The resulting classifier will be specific for an FP type and is then applied to all datasets.

## Results and Discussion

OCSVM was trained on cortical ROIs in images of 2 month old 5xFAD mouse brains (n=2). For TCSVM training (Figure 1), we used ROIs in caudate putamen (striatum) for cylinder FPs and hippocampal fimbria for interface FPs of 10 month old excised 5xFAD mouse brains (n=2). The algorithm was evaluated by cross validation, so that the TCSVM classifier trained on a 10 M mouse brain was applied to the other 10 M mouse brain in the cortex ROI (with plaques but no FPs) and the ROI with FP samples (striatum for the cylinder TCSVM classifier and fimbria for the interface TCSVM classifier). Sensitivity was estimated by computing the percentage of FP labeled CBs in the striatum for the cylinder classifier, and a manually delineated ground truth for interface classifier. Specificity was estimated by the percentage of FP labeled CBs in the cortex. Results of the FP TCSVM training are shown in Figure 2. Because the feature space is 5D we can only show 2D sections that not always cross the classification function displayed in red. The area under the ROC curve ( $A_{ROC}$ ) was estimated by using the average sensitivity and specificity values computed for the cross-validation datasets.  $A_{ROC}$  values were 0.898 for the cylinder SVM, and 0.832 for the interface SVM. Figure 3 shows examples of segmented plaques. Our approach is novel since it does not require supervised training, and we did not follow the common approach of computing specific functions describing the "sheetness" or "vesselness" of a CB. Instead, we use the SVM flexibility of computing non-linear classification functions that can be used to detect FPs of specific shape. Our results show that our unsupervised algorithm is flexible and can be extended to reduce plaque detection FPs in MR images of AD mouse models, making our method suitable for the analysis of individual plaques and plaque distribution within different brain structures.

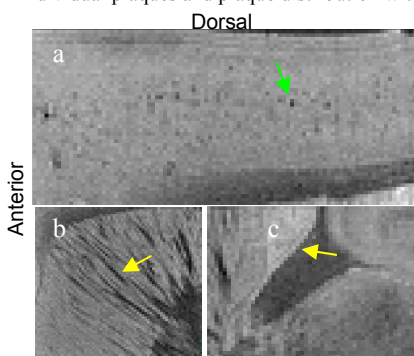


**Figure 1**  
Sagittal MR images of cortex (a), striatum (b) and fimbria (c) of a 10 month old 5xFAD mouse brain. Hypointense areas correspond to plaques in cortex (green arrow) and cylinders (yellow arrow) in striatum. Fimbria interfaces (yellow arrow) were manually delineated for validation.

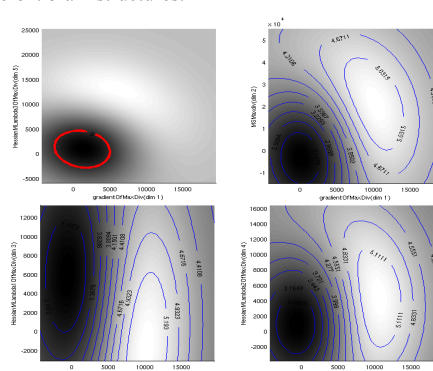


**Figure 2**  
Cylinder FP TCSVM classifier: Sections through the 5D classification function (red curve) are superimposed on its distance space with isocontours displayed in blue.

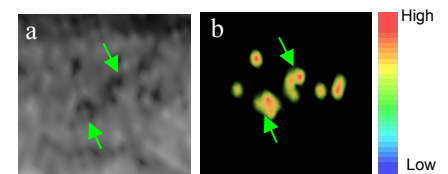


**Figure 3**  
MR image (a) and corresponding segmented plaque (b) of a 10 month old 5xFAD mouse brain. Segmented plaques are displayed in pseudo-color volume-rendering of the new multiscale Laplacian values. Plaques locations and their corresponding detections are indicated by a linked cursor (green arrows)

1. Vincent L, et al. IEEE Trans PAMI 13/6: 583-598, 1991
2. Vapnik V. N., Statistical Learning Theory. Wiley, 1998
3. Oakley H., et al. J. Neurosci. 26: 10129-140, 2006
4. Scholkopf B., et al. Neural Computation, 13(7):1443-1471, 2001
5. Chang C. C., et al., LIBSVM: a library for support vector machines, 2001. Software available at <http://www.csie.ntu.edu.tw/~cjlin/libsvm>

Acknowledgement: NIH RO1 AG 027424